NeRF-HuGS: Improved Neural Radiance Fields in Non-static Scenes Using Heuristics-Guided Segmentation

Jiahao Chen[1] Yipeng Qin[2] Lingjie Liu[3] Jiangbo Lu[4] Guanbin Li[1*]
[1]Sun Yat-sen University [2]Cardiff University [3]University of Pennsylvania [4]SmartMore Corporation
chenjh328@mail2.sysu.edu.cn, qiny16@cardiff.ac.uk, lingjie.liu@seas.upenn.edu
jiangbo.lu@gmail.com, liguanbin@mail.sysu.edu.cn

Abstract

Neural Radiance Field (NeRF) has been widely recognized for its excellence in novel view synthesis and 3D scene reconstruction. However, their effectiveness is inherently tied to the assumption of static scenes, rendering them susceptible to undesirable artifacts when confronted with transient distractors such as moving objects or shadows. In this work, we propose a novel paradigm, namely "Heuristics-Guided Segmentation" (HuGS), which significantly enhances the separation of static scenes from transient distractors by harmoniously combining the strengths of hand-crafted heuristics and state-of-the-art segmentation models, thus significantly transcending the limitations of previous solutions. Furthermore, we delve into the meticulous design of heuristics, introducing a seamless fusion of Structure-from-Motion (SfM)-based heuristics and color residual heuristics, catering to a diverse range of texture profiles. Extensive experiments demonstrate the superiority and robustness of our method in mitigating transient distractors for NeRFs trained in non-static scenes. Project page: https://cnhaox.github.io/NeRF-HuGS/

1. Introduction

Neural Radiance Fields (NeRF) [29] have garnered significant attention for their remarkable achievements in novel view synthesis. Utilizing multiple-view images, NeRF conceptualizes the 3D scene as a neural field [54] and produces highly realistic renderings through advanced volume rendering techniques. This capability has opened the door to a wide array of downstream applications including 3D reconstruction [22, 43, 48], content generation [23, 33, 36], semantic understanding [14, 42, 58], etc.

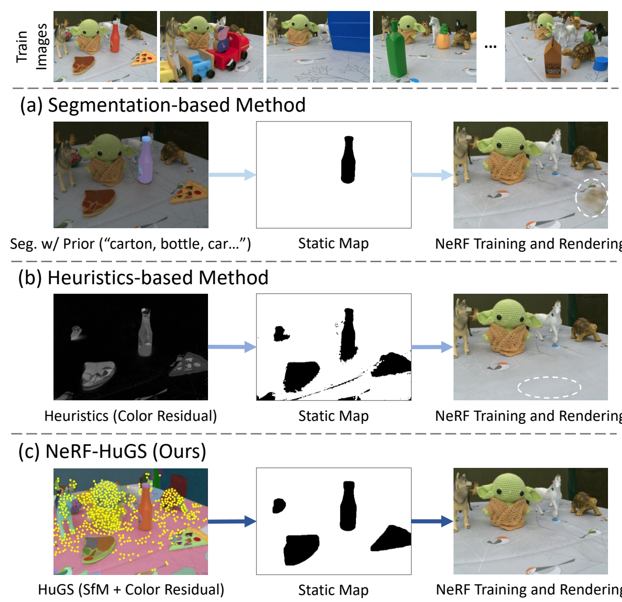

Figure 1. **Comparison between previous methods and the proposed Heuristics-Guided Segmentation (HuGS) paradigm.** When training NeRF with static scenes disturbed by transient distractors, (a) segmentation-based methods rely on prior knowledge and cannot identify unexpected transient objects (*e.g.*, pizza); (b) heuristics-based methods are more generalizable but inaccurate (*e.g.*, tablecloth textures); (c) our method combines their strengths and produces highly accurate transient *vs.* static separations, thereby significantly improving NeRF results.

However, the images used as NeRF training data must meet several strict conditions, one of which is the requirement for content consistency and stability. In other words, the native NeRF model operates under the assumption of a static scene. Any elements that exhibit motion or inconsistency throughout the entire data capture session, which we refer to as "*transient distractors*", can introduce undesirable artifacts into the reconstructed 3D geometry. However, the presence of transient distractors is nearly inevitable in real-world scenarios. For instance, in outdoor settings, random appearances of pedestrians and vehicles may occur during

*Corresponding author is Guanbin Li. This work was supported in part by the National Natural Science Foundation of China (NO. 62322608), in part by the CAAI-MindSpore Open Fund, developed on OpenI Community, in part by the Open Project Program of State Key Laboratory of Virtual Reality Technology and Systems, Beihang University (No.VRLAB2023A01), in part by Shenzhen Science and Technology Program KQTD20210811090149095 and also the Pearl River Talent Recruitment Program 2019QN01X226.

image acquisition, while indoor shooting may be affected by shadows cast by the photographer. Furthermore, manually removing these transient distractors from a substantial number of images is a challenging and time-consuming task, often necessitating pixel-by-pixel labeling.

To mitigate the effects of transient distractors, previous research has explored two main paradigms. One paradigm involves leveraging pre-trained segmentation models to detect transient distractors [12, 26, 38, 43, 45, 47]. Although it can produce accurate results, this approach exhibits limited generality as it relies on additional prerequisites of prior knowledge (*e.g.*, semantic classes of transient objects). The other strategy aims to separate transient distractors from static scenes through the application of hand-crafted heuristics [7, 15, 17, 18, 28, 40]. Nonetheless, this approach often yields imprecise or erroneous results, primarily attributed to the intricate nature of heuristic design and the inherent ill-posedness of existing heuristics.

In this work, we take the best of both worlds and propose a novel paradigm called "*Heuristics-Guided Segmentation*" (HuGS) to maximize the accuracy of static *vs.* transient object identification for NeRF in non-static scenes (Fig. 1). The rationale of our approach lies in the principle embodied in the British idiom "horses for courses", emphasizing the alignment of talents with tasks. Specifically, our paradigm harnesses the collective strengths of i) hand-crafted heuristics, adept at discerning rough indicators of static elements, and ii) contemporary segmentation models, like the Segment Anything Model (SAM) [16] renowned for their ability to delineate precise object boundaries. Furthermore, we delve deeply into the design of heuristics and suggest a seamless fusion of i) our newly devised Structure-from-Motion (SfM)-based heuristics, which efficiently identify static objects characterized by high-frequency texture patterns, with ii) the color residual heuristics derived from a partially trained Nerfacto [46], which excel at detecting static elements marked by low-frequency textures. This tailored integration of heuristics empowers our method to robustly encompass the full spectrum of static scene elements across a diverse range of texture profiles. Extensive experiments have demonstrated the superiority of our method. Our contributions can be summarized as follows:

- We propose a novel paradigm called "Heuristics-Guided Segmentation" for improving NeRF trained in non-static scenes, which takes the best of both hand-crafted heuristics and state-of-the-art segmentation models to accurately distinguish static scenes from transient distractors.
- We delve into heuristic design and propose the seamless fusion of SfM-based heuristics and color residual ones to capture a wide range of static scene elements across various texture profiles, offering robust performance and superior results in mitigating transient distractors.
- Extensive experimental results show that our method produces sharp and accurate static *vs.* transient separation results close to the ground truth, and significantly improves NeRFs trained in non-static scenarios.

2. Related Work

NeRF [29] has recently emerged as a promising solution to synthesizing novel photo-realistic views from multiple images, which is a long-standing problem in computer vision. Although numerous methods [1–3, 32, 56] have been proposed to improve its synthesis quality and training efficiency, most of them assume that the scenes to be reconstructed are static and are therefore not suitable for many real-world scenes (*e.g.*, tourist attractions).

NeRF in Non-static Scenes. In general, there are two major types of non-static scenes that present challenges for NeRF: i) Dynamic scenes that change over time, where the model needs to render consistent novel views of the scene as it evolves [10, 19, 21, 26, 34, 35, 53], *e.g.*, scenes with moving objects or environmental effects like lighting or weather changes. ii) Static scenes disturbed by transient distractors, where the model should exclude dynamic objects like tourists walking through static attractions as background scenes. Our work focuses on ii), where existing solutions can be roughly grouped into two main paradigms:

- *Segmentation-based methods* [12, 26, 38, 43, 45, 47] use pre-trained semantic or video segmentation models to identify transient distractors *vs.* static scenes and use the information obtained to facilitate NeRF training. These models can produce accurate results but have some key limitations: i) They require additional priors like the semantic class of transient distractors or the temporal relationships of the images as video frames, which are hard to satisfy in practice as it is intractable to enumerate all possible distractor classes, and images may be unordered. ii) Semantic segmentation cannot distinguish between static and transient objects of the same class.
- *Heuristics-based methods* [7, 15, 17, 18, 28, 40] use hand-crafted heuristics to separate transient distractors from static scenes during NeRF training, making themselves more generalizable as they require no prior. However, heuristics that enable accurate separation are difficult to design. For example, NeRF-W [28] observes that the density of transient objects is usually small and uses this to regularize NeRF training. However, it can easily produce foggy residuals with small densities that are not transient objects. RobustNeRF [40] distinguishes transient pixels from static ones through color residuals as transient pixels are more difficult to fit during NeRF training. However, high-frequency details of static objects are also difficult to fit, causing RobustNeRF to easily ignore them when dealing with transient distractors.

In our work, we propose a new paradigm called HuGS that

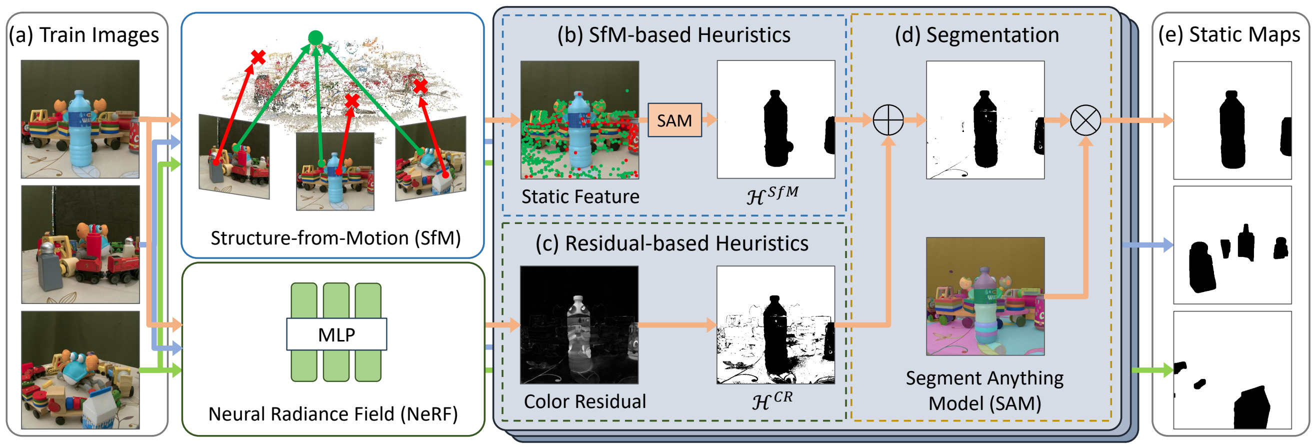

Figure 2. **Pipeline of HuGS.** (a) Given unordered images of a static scene disturbed by transient distractors as input, we first obtain two types of heuristics. (b) SfM-based heuristics use SfM to distinguish between static (green) and transient features (red). The static features are then employed as point prompts to generate dense masks using SAM. (c) Residual-based heuristics are based on a partially trained NeRF (*i.e.*, trained for several thousands of iterations) that can provide reasonable color residuals. (d) Their combination finally guides SAM again to generate (e) the static map for each input image.

takes the best of both worlds. In short, we match talents to tasks and propose to use heuristics only as rough cues to guide the segmentation and produce highly accurate transient *vs.* static separations that are close to the ground truth. We also investigate heuristics design and propose to use a combination of heuristics based on color residuals and SfM.

SfM in NeRF. SfM is a technique for reconstructing the corresponding 3D geometry from a set of 2D images. In NeRF, SfM is typically used to estimate the camera pose of an image. Recent works have also used it to estimate the scene depth [43], locate target objects [49, 55] or initialize the set of 3D Gaussians [13]. In addition to estimating camera poses, our method also uses SfM to design novel heuristics for static *vs.* transient object identification. Specifically, we leverage the insight that only feature points belonging to static scene elements can be reliably matched and triangulated across multiple views in the SfM pipeline. To the best of our knowledge, we are the first to exploit this property of SfM for NeRF in non-static scenes.

3. Preliminaries

Let $\mathcal{I} = \{I_i \mid i = 1, 2, \ldots, N_I\}$ be a set of multi-view input images with transient objects, we have:

Structure-from-Motion (SfM). SfM first extracts a set of 2D local feature points $\mathcal{F}_i$ for each I_i:

$$\mathcal{F}_i = \left\{ \left(\mathbf{x}_i^j, \mathbf{f}_i^j \right) \mid j = 1, 2, \ldots, N_{F_i} \right\}, \tag{1}$$

where $\mathbf{f}_i^j$ is an appearance descriptor and $\mathbf{x}_i^j \in \mathbb{R}^2$ denotes its coordinates in I_i. Then, SfM uses the $\mathcal{F}_i$ of all images to reconstruct a sparse point cloud $\mathcal{C}$ representing the 3D structure of the target scene, where the correspondence between 2D feature points (*i.e.*, *matching* points) in different images is determined by whether or not they correspond to the same 3D point in $\mathcal{C}$. For each 2D feature point $\left(\mathbf{x}_i^j, \mathbf{f}_i^j\right)$, we denote the number of its *matching* points in $\mathcal{I}$ as n_i^j.

Neural Radiance Field (NeRF). In short, NeRF represents a static scene with a multi-layer perceptron (MLP) parameterized by $\boldsymbol{\theta}$. Specifically, given a 3D position $\mathbf{p} \in \mathbb{R}^3$ and its viewing direction $\mathbf{d} \in \mathbb{S}^2$, NeRF outputs its corresponding color $\mathbf{c} \in \mathbb{R}^3$ and density $\sigma \in \mathbb{R}$ as:

$$(\mathbf{c}, \sigma) = \text{MLP}(\mathbf{p}, \mathbf{d}; \boldsymbol{\theta}). \tag{2}$$

This allows NeRF to render each pixel color $\hat{\mathbf{C}}(\mathbf{r})$ in a 2D projection by applying volume rendering along its corresponding camera ray $\mathbf{r}$ with multiple sample points. During training, the parameters $\boldsymbol{\theta}$ are optimized by minimizing the error between $\hat{\mathbf{C}}(\mathbf{r})$ and the ground truth color $\mathbf{C}(\mathbf{r})$ in input images using loss function:

$$\mathcal{L}(\mathbf{r}) = \mathcal{L}_{\text{recon}}(\hat{\mathbf{C}}(\mathbf{r}), \mathbf{C}(\mathbf{r})), \tag{3}$$

where $\mathcal{L}_{\text{recon}}$ is a reconstruction loss whose popular choices include the MSE loss and the Charbonnier loss [5].

NeRF in Static Scenes. Let M_i be the static map corresponding to image I_i which labels pixels of transient objects with 0 and pixels of static objects with 1, we modify Eq. 3 in a straightforward way by using M_i as the loss weight to avoid the interference of transient pixels:

$$\mathcal{L}(\mathbf{r}) = M(\mathbf{r}) \mathcal{L}_{\text{recon}}(\hat{\mathbf{C}}(\mathbf{r}), \mathbf{C}(\mathbf{r})), \tag{4}$$

where we omit i and use $\mathbf{r}$ instead for simplicity.

4. Method

As Eq. 4 implies, the more accurate the static maps M_i are, the higher the quality of the trained NeRF. To max-

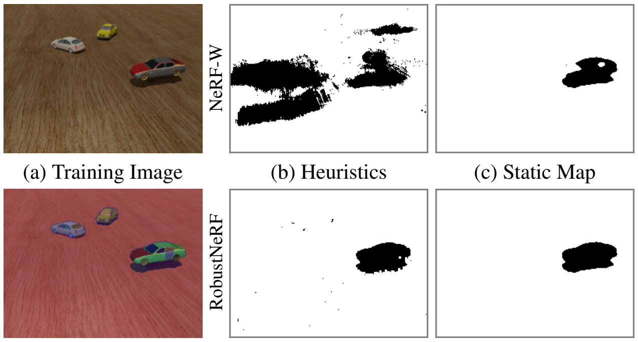

(a) Training Image (b) Heuristics (c) Static Map

(d) Seg. Masks (e) Heuristics (f) Static Map

Figure 3. **Performance of HuGS using existing heuristics.** (a) is an example training image with a moving red car, and (d) is its segmentation result using SAM. (b, e) are heuristic maps obtained from different partially trained models. (c, f) are static maps produced by our method, where inaccurate heuristics may lead to incorrect results (NeRF-W).

imize the accuracy of M_i, we follow the British idiom "horses for courses", which suggests matching talents to tasks, and approach the problem through a novel framework called *Heuristics-Guided Segmentation (HuGS)* (Sec. 4.1). As Fig. 2 shows, HuGS combines the strengths of both hand-crafted heuristics in identifying coarse cues of static objects and the capabilities of state-of-the-art segmentation models in producing sharp and accurate object boundaries. Furthermore, we conduct an in-depth analysis of the choice of heuristics (Sec. 4.2). Our solution combines novel SfM-based heuristics, which effectively identify static objects with high-frequency texture patterns, with the color residual heuristics from a partially trained Nerfacto [46], which excel at detecting static objects characterized by low-frequency textures. This tailored integration of heuristics allows our method to robustly capture the full range of static scene elements across diverse texture profiles.

4.1. Heuristics-Guided Segmentation (HuGS)

While humans can easily distinguish between transient and static objects, providing a rigorous mathematical definition of this distinction has proven elusive thus far due to the high diversity of real-world scenes. To this end, the most effective existing solutions rely heavily on hand-crafted heuristics to make this distinction. For example, NeRF-W [28] employs the heuristics that transient objects usually have lower density than their static counterparts and incorporates this as a regularization term during NeRF training; RobustNeRF [40] leverages the observation that transient objects are typically harder to fit during optimization and uses it to produce the static maps used in Eq. 4. However, despite their success, these methods implicitly make the strong assumption that distinguishing between transient and static rays/pixels can be determined *solely* based on simple hand-crafted heuristics, which does not hold up while handling the diverse shapes and appearances of real-world objects. As a result, these methods are prone to produce errors and/or ambiguous object boundaries (Figs. 3b and 3e).

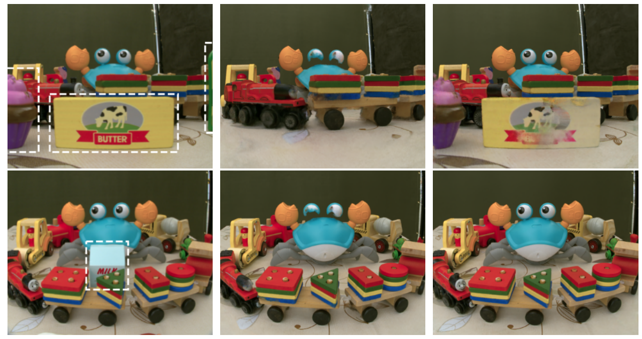

(a) Training Image (b) Quantile = 0.7 (c) Quantile = 0.9

Figure 4. **Performance of RobustNeRF *vs.* transient objects of different sizes.** Transient distractors in the training images are framed in white. A lower quantile (threshold) causes the model to miss small-sized static objects, while a higher quantile prevents the removal of large-sized transient objects.

To address this limitation, we propose a novel framework HuGS that avoids fully relying on hand-crafted heuristics to differentiate between transient and static objects. Instead, our approach leverages heuristics to provide *only* rough hints $\mathcal{H}_i$ about potential static objects in each image I_i, and then refines those imprecise cues into accurate static maps M_i using the segmentation masks of I_i provided by model S. Specifically, let $S(I_i) = \{m_i^1, m_i^2, ..., m_i^{N_{M_i}}\}$, where m_i^j denotes the segmentation mask of the j-th object (instance) and N_{M_i} is the number of masks, we have:

$$M_i = \bigcup m_i^j, \ \forall \frac{m_i^j \cap \mathcal{H}_i}{m_i^j} \geq \mathcal{T}_m, \tag{5}$$

where $\mathcal{T}_m$ is a user-specified threshold and we implement S using the state-of-the-art SAM [16]. As shown in Fig. 3, our framework can produce static maps with sharp object boundaries even when using partially trained (10%) models of previous methods [28, 40] as heuristics (Figs. 3b and 3e). However, despite the relaxation, the success of our framework is based on the assumption that rough but accurate $\mathcal{H}_i$ about static objects are available (Figs. 3c and 3f).

4.2. Heuristics Development

To provide rough but accurate heuristics $\mathcal{H}_i$ of static objects, we use a combination of two complementary heuristics, *i.e*. our novel SfM-based heuristics and the color residual heuristics from a partially trained Nerfacto [46], which excel in detecting statics objects with high-frequency and low-frequency textures respectively.

SfM-based Heuristics. As mentioned above in Sec. 3, SfM reconstruction relies on matching distinct, identifiable features across images. This makes it well-suited for detect-

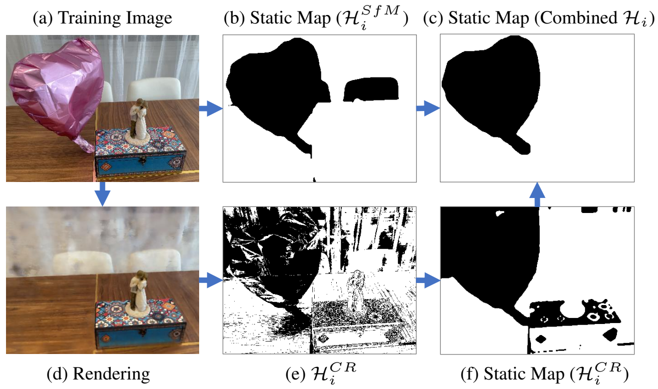

Figure 5. **Heuristics combination.** (b) The SfM-based heuristics $\mathcal{H}_i^{SfM}$ alone captures high-frequency static details (*e.g.*, box textures) well but misses smooth ones (*e.g.*, white chairs). This could be complemented by incorporating (e) residual-based heuristics $\mathcal{H}_i^{CR}$ from a (d) Nerfacto with $5k$ training iterations which does the opposite (f). Their combination (c) covers the full spectrum of static scenes and identifies transient objects (*e.g.*, pink balloon).

ing objects characterized by high-frequency textures, since these distinctive textures provide abundant unique features to match. To distinguish between static and transient objects, our SfM-based heuristics share a similar high-level intuition to previous methods in that transient objects are considered a minority compared to static ones and their positions are constantly changing. However, ours has a different interpretation of "minority". Specifically, our method defines it as the *frequency of occurrence* across input images, which aligns well with the temporal meaning of "transient". In contrast, NeRF-W [28] and RobustNeRF [40] interpret "minority" in terms of total density or quantile of color residual respectively, which relate more to *spatial area coverage*. As a result, their methods struggle with transient objects of varying sizes (Fig. 4), since the area-based definitions do not fully capture the temporal aspect of identifying transient objects. Recalling the definition of n_i^j (the number of matching points) and N_I (the number of input images) in Sec. 3, we have the following observation:

Observation 1. *The SfM features of static objects have much larger n_i^j than those of transient ones in image I_i.*

Note that the already smaller n_i^j of transient objects could be further reduced by their constantly changing positions (*i.e.*, less likely to get matched during SfM reconstruction), making them easier to distinguish. Accordingly, we set a threshold $\mathcal{T}_{SfM}$ to obtain set $\mathcal{X}_i$ of the coordinates of static feature points for each image I_i:

$$\mathcal{X}_i = \left\{ \mathbf{x}_i^j \;\middle|\; \mathbf{x}_i^j \in \mathcal{F}_i \text{ and } \frac{n_i^j}{N_I} \geq \mathcal{T}_{SfM} \right\}. \tag{6}$$

where we set $\mathcal{T}_{SfM}$ based on $\frac{n_i^j}{N_I}$ rather than n_i^j as the former better represents the *frequency of occurrence* across the whole scene. However, $\mathcal{X}_i$ is a relatively sparse point set, so we need to convert it to a pixel-wise static map for NeRF training. Fortunately, SAM [16] is a promptable segmentation model that can accept points as prompts and output their corresponding segmentation masks. Therefore, we feed $\mathcal{X}_i$ into SAM to obtain heuristics $\mathcal{H}_i^{SfM}$, which is a static map where a pixel value of 1 means that it belongs to a static object and 0 means that it is a transient one.

Combined Heuristics. Although effective, our SfM-based heuristics $\mathcal{H}^{SfM}$ may neglect low-frequency static objects due to their lack of distinctive features (Fig. 5). To address this limitation, we propose an integrated approach that incorporates the complementary strength of another heuristic: the color residual of a partially trained Nerfacto [46], which effectively identifies smooth transient objects but struggles with textured objects. Specifically, we first train a Nerfacto for several thousands of iterations and construct its color residual map $\mathcal{R}_i$ using the color residual for each ray $\mathbf{r}$ as $\epsilon(\mathbf{r}) = \|\hat{\mathbf{C}}(\mathbf{r}) - \mathbf{C}(\mathbf{r})\|_2$. We then combine $\mathcal{H}_i^{SfM}$ with residual-based heuristics $\mathcal{H}_i^{CR}$ to get heuristics $\hat{\mathcal{H}}_i$:

$$\hat{\mathcal{H}}_i = \mathcal{H}_i^{SfM} \cup \mathcal{H}_i^{CR}, \tag{7}$$

where $\mathcal{H}_i^{CR} = \mathcal{R}_i \leq \text{mean}(\mathcal{R}_i)$. While in practice, our $\mathcal{H}_i^{SfM}$ may occasionally incorrectly include some transient objects due to misclassification of feature points or SAM segmentation errors. To eliminate them, we apply an upper bound defined by $\hat{\mathcal{H}}_i^{CR}$ to Eq. 7 as additional insurance:

$$\mathcal{H}_i = \hat{\mathcal{H}}_i \cap \hat{\mathcal{H}}_i^{CR}, \tag{8}$$

where $\hat{\mathcal{H}}_i^{CR} = \mathcal{R}_i \leq \text{quantile}(\mathcal{R}_i, \mathcal{T}_{CR})$. $\mathcal{T}_{CR}$ is a high threshold that ensures $\hat{\mathcal{H}}_i^{CR}$ include all static objects.

Remark. We use Nerfacto [46] to generate residual maps as it can be trained quickly with much fewer computational resources and still producing reasonable results (Fig. 5). Although relatively low, this level of performance is sufficient to satisfy our requirement for rough heuristic cues, which further demonstrates the superiority of our paradigm.

5. Experiments

5.1. Experimental Setup

Datasets. We use three datasets in our experiments:

- *Kubric Dataset [53].* Generated by Kubric [11], this synthetic dataset contains five scenes with simple geometries placed in an empty room. The frames have temporal relationships and a subset of geometries serves as transient distractors that move between frames.
- *Distractor Dataset [40].* This real-world dataset has four controlled indoor scenes with 1-150 distractors per scene.
- *Phototourism Dataset [28].* This real-world dataset has scenes of four cultural landmarks, each with photos collected online containing various transient distractors. The

Method	Car			Cars			Bag			Chairs			Pillow			Avg.		
	PSNR↑	SSIM↑	LPIPS↓	PSNR↑	SSIM↑	LPIPS↓	PSNR↑	SSIM↑	LPIPS↓	PSNR↑	SSIM↑	LPIPS↓	PSNR↑	SSIM↑	LPIPS↓	PSNR↑	SSIM↑	LPIPS↓
Nerfacto [46]	30.71	.862	.227	29.50	.809	.316	31.32	.917	.103	27.41	.811	.258	29.86	.906	.148	29.76	.861	.210
Mip-NeRF 360 [2]	26.67	.846	.238	28.88	.822	.281	32.81	.948	.053	27.07	.839	.179	29.66	.919	.123	29.02	.875	.175
NeRF-W [28]	29.44	.901	.124	28.34	.867	.186	34.49	.946	.045	22.75	.826	.187	29.04	.915	.142	28.81	.891	.137
HA-NeRF [7]	28.69	.915	.124	31.95	.903	.143	38.48	.969	**.021**	33.48	.922	.071	31.66	.946	.083	32.85	**.931**	.089
D^{2}NeRF [53]	34.03	.874	.099	33.67	.844	.123	33.77	.889	.118	32.77	.875	.113	29.49	.907	.139	32.75	.878	.118
RobustNeRF [40]	**37.31**	**.968**	**.040**	**40.52**	**.963**	**.047**	**40.50**	**.976**	.026	**38.56**	**.958**	**.037**	**41.31**	**.980**	**.028**	**39.64**	**.969**	**.036**
Ours (Nerfacto)	**39.49**	**.964**	**.042**	**39.95**	**.958**	**.045**	**41.39**	**.980**	**.017**	**38.48**	**.962**	**.036**	**42.70**	**.982**	**.025**	**40.40**	**.969**	**.033**
Ours (Mip-NeRF 360)	**39.75**	**.972**	**.036**	**40.74**	**.966**	**.046**	**42.32**	**.983**	**.019**	**39.32**	**.968**	**.033**	**43.90**	**.986**	**.023**	**41.21**	**.975**	**.032**

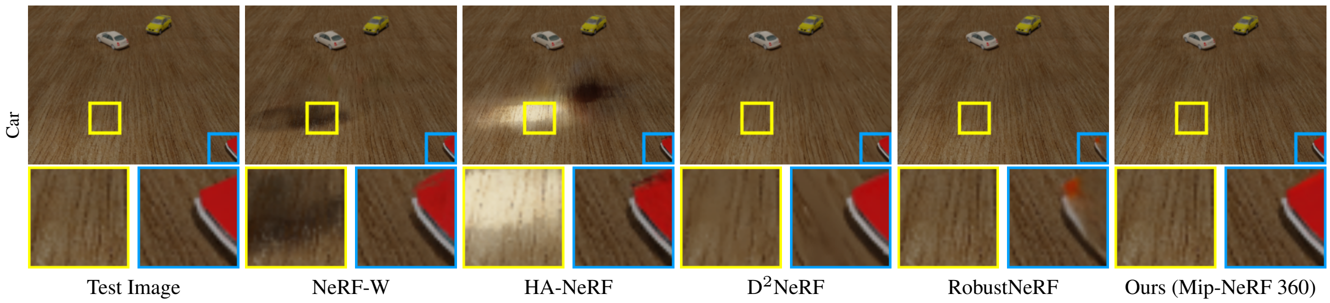

Figure 6. **Quantitative and qualitative results on the Kubric dataset.** The 1st, 2nd and 3rd best results are highlighted. Quantitatively, our method not only significantly improves the performance of Nerfacto and Mip-NeRF 360, but also helps Mip-NeRF 360 outperform the previous methods and become the SOTA. Qualitatively, our method can better preserve static details while ignoring transient distractors.

Method	Statue			Android			Crab			BabyYoda			Avg.		
	PSNR↑	SSIM↑	LPIPS↓	PSNR↑	SSIM↑	LPIPS↓	PSNR↑	SSIM↑	LPIPS↓	PSNR↑	SSIM↑	LPIPS↓	PSNR↑	SSIM↑	LPIPS↓
Nerfacto [46]	18.21	.591	.336	21.34	.617	.226	26.62	.864	.135	22.06	.697	.267	22.06	.692	.241
Mip-NeRF 360 [2]	**19.86**	.690	.233	21.81	.695	.176	29.25	.918	.086	23.75	.770	.216	23.67	.768	.178
NeRF-W [28]	18.91	.616	.369	20.62	.664	.258	26.91	.866	.157	28.64	.752	.260	23.77	.725	.261
HA-NeRF [7]	18.67	.616	.367	22.03	.706	.203	28.58	.901	.116	**29.28**	.779	.208	24.64	.750	.224
RobustNeRF [40]	**20.60**	**.758**	**.154**	**23.28**	**.755**	**.126**	**32.22**	**.945**	**.060**	**29.78**	**.821**	**.155**	**26.47**	**.820**	**.124**
Ours (Nerfacto)	19.18	**.703**	**.183**	**22.59**	**.720**	**.120**	**32.11**	**.939**	**.033**	28.77	**.802**	**.087**	**25.66**	**.791**	**.106**
Ours (Mip-NeRF 360)	**21.00**	**.774**	**.135**	**23.32**	**.763**	**.123**	**34.16**	**.956**	**.032**	**30.70**	**.834**	**.124**	**27.29**	**.832**	**.103**

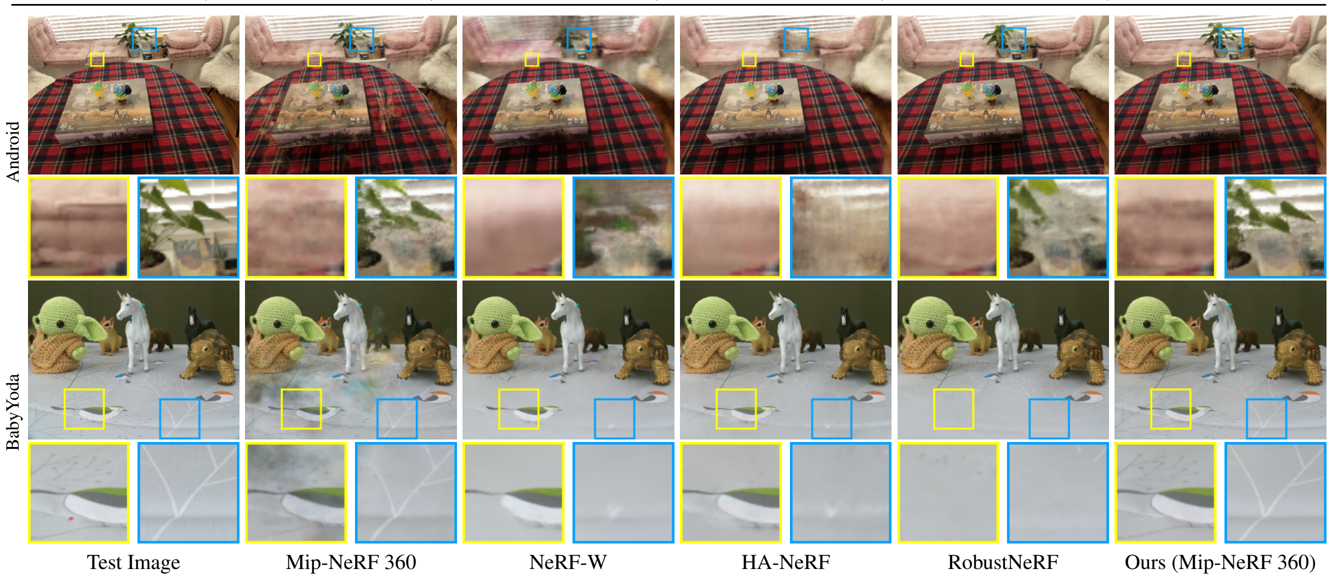

Figure 7. **Quantitative and qualitative results on the Distractor dataset.** The 1st, 2nd and 3rd best results are highlighted. Our method applied to Mip-NeRF 360 is the best in most quantitative results, with our method applied to Nerfacto leading the rest. Qualitatively, our method captures scene details better compared to other baselines, which suffer from missing or disturbed details.

Method	Brandenburg Gate			Sacre Coeur			Taj Mahal			Trevi Fountain			Avg.		
	PSNR↑	SSIM↑	LPIPS↓	PSNR↑	SSIM↑	LPIPS↓	PSNR↑	SSIM↑	LPIPS↓	PSNR↑	SSIM↑	LPIPS↓	PSNR↑	SSIM↑	LPIPS↓
Nerfacto [46]	24.69	.890	.132	21.09	.819	.169	22.80	.804	.237	22.63	.748	.195	22.80	.815	.183
Mip-NeRF 360 [2]	25.59	.904	.121	21.46	.818	.175	24.33	.828	.202	23.25	.767	.189	23.66	.829	.172
NeRF-W [28]	23.62	.851	.171	19.75	.749	.233	22.23	.772	.317	20.80	.664	.299	21.60	.759	.255
HA-NeRF [7]	23.93	.881	.140	19.85	.808	.175	20.70	.811	.234	20.07	.713	.223	21.14	.803	.193
RobustNeRF [40]	25.79	.923	.094	20.94	.852	.137	24.64	.859	.173	23.58	.785	.170	23.73	.855	.144
Ours (Nerfacto)	25.99	.919	.087	22.03	.856	.132	24.06	.836	.198	22.90	.770	.173	23.74	.845	.147
Ours (Mip-NeRF 360)	27.17	.929	.083	22.23	.862	.124	24.92	.857	.176	23.41	.788	.165	24.43	.859	.137

Trevi Fountain

Test Image Mip-NeRF 360 NeRF-W HA-NeRF RobustNeRF Ours (Mip-NeRF 360)

Figure 8. **Quantitative and qualitative results on the Phototourism dataset.** The 1st, 2nd and 3rd best results are highlighted. Note that the main content of test images in this dataset is the upper part of the building, which is less affected by transient distractors (*e.g.*, tourists). Thus, our method brings less improvement but still yields competitive results against the SOTA.

landmark and distractor appearances vary across images due to shooting differences.

Implementation Details. Please see the supplementary materials for more details.

- *HuGS.* We use COLMAP [41] for SfM reconstruction and SAM [16] as the segmentation model. COLMAP uses SIFT [27] to extract image features, and we set COLMAP's parameters to default values. We set $\mathcal{T}_m$ to a common 0.5. The values of $\mathcal{T}_{SfM}$ and $\mathcal{T}_{CR}$ depend on the complexity of the scene, so we empirically set them to 0.2 and 0.9 for Kubric, 0.01 and 0.95 for Distractor, 0.01 and 0.97 for Phototourism datasets.
- *NeRF Training.* We apply our method to two baseline NeRF models, Nerfacto [46] and Mip-NeRF 360 [2], to show its generalizability. We did not test it on the vanilla NeRF [29] because the vanilla NeRF has difficulty handling the unbounded scenes in the Distractor dataset [2].

5.2. Evaluation on View Synthesis

Baselines. In addition to baseline models, we compare our method to three other state-of-the-art heuristics-based methods: NeRF-W [28], HA-NeRF [7] and RobustNeRF [40], which design heuristics based on scene density, pixel visible possibility, and color residuals, respectively. We also compare our method to D^{2}NeRF [53] on the Kubric dataset, which is a dynamic NeRF that works well on monocular videos. Segmentation-based methods are not included in our comparison because they rely on priors of transient distractors, which cannot be satisfied in most scenes.

Comparisons. Both the above models and ours are trained on images disturbed by transient distractors and evaluated on images with only static scenes. We report image synthesis qualities based on PSNR, SSIM [50] and LPIPS [57].

- *Kubric dataset* (Fig. 6). Compared to the native ones, applying our method leads to substantial PSNR improvements of 8.78 to 12.84dB for Nerfacto, and 9.51 to 14.24dB for Mip-NeRF 360. Our method achieves this by generating high-quality static maps that effectively shield the native models from pixels disturbed by transient distractors. Compared to the other baselines, our method achieves the highest quantitative results and maintains a good balance between ignoring transient distractors and preserving static details. Specifically, NeRF-W and HA-NeRF fail due to incorrect decoupling of transient distractors from the static scenes; D^{2}NeRF and RobustNeRF achieve better decoupling but lose static details such as ground textures and the red car.
- *Distractor dataset* (Fig. 7). The results and conclusions are similar to those on the Kubric dataset.
- *Phototourism dataset* (Fig. 8). Its training and test sets share a unique feature: the landmark *main bodies* are not deeply disturbed by transient distractors (*e.g.* nearby tourists) and can be well reconstructed even without the removal of transient distractors. Thus, the improvement from our method mainly focus on the landmark *boundaries* and is relatively less compared to the above datasets. Nonetheless, our results remain quantitatively competitive and qualitatively recover more details compared to prior works. Please see the supplement for more details.

5.3. Evaluation on Segmentation

Baselines. We perform the comparison on the Kubric dataset, which is synthetic and has ground truth segmen-

Method	Seg. Type	Require Prior	Car mIoU↑	Car F1↑	Cars mIoU↑	Cars F1↑	Bag mIoU↑	Bag F1↑	Chairs mIoU↑	Chairs F1↑	Pillow mIoU↑	Pillow F1↑	Avg. mIoU↑	Avg. F1↑
DeepLabv3+ [6]	*Semantic*	✓	.604	.378	.578	.293	.501	.048	.564	.239	.535	.149	.556	.221
Mask2Former [8]	*Semantic*	✓	.664	.520	.622	.376	.513	.071	.707	.561	.653	.377	.632	.381
Grounded-SAM [16, 25]	*Open-Set*	✓	.888	.877	.640	.406	.755	.671	.603	.373	**.851**	**.828**	.747	.631
DINO [4]	*Video*	✓	**.947**	**.947**	.720	.557	.591	.367	**.777**	**.703**	**.911**	**.904**	.789	.695
NeRF-W [28]	/	✗	.682	.575	.584	.328	.526	.099	.547	.298	.557	.296	.579	.319
HA-NeRF [7]	/	✗	.869	.852	**.823**	**.724**	**.813**	**.771**	.729	.595	.819	.766	**.811**	**.742**
D^{2}NeRF [53]	/	✗	**.912**	**.909**	**.895**	**.867**	**.794**	**.727**	.660	.507	.800	.760	**.812**	**.754**
RobustNeRF [40]	/	✗	.813	.784	.718	.547	.731	.633	**.731**	**.638**	.724	.633	.743	.647
HuGS (Ours)	/	✗	**.963**	**.964**	**.940**	**.907**	**.939**	**.935**	**.937**	**.927**	**.940**	**.937**	**.944**	**.934**

Training Image GT Mask2former DINO HA-NeRF D^{2}NeRF RobustNeRF Ours

Figure 9. **Quantitative and qualitative segmentation results on the Kubric dataset.** The **1st**, **2nd** and **3rd** best results are highlighted.

tation data. We compare our method with various existing segmentation models, including semantic segmentation models [6, 8], open-set segmentation models [16, 25] and video segmentation models [4]. The baseline NeRF models mentioned above are also compared by using the static maps generated after they are fully trained.

Comparisons (Fig. 9). We report segmentation qualities based on the mIoU and F1 score. Interestingly, we observe that even when prior knowledge is provided, the performance of existing segmentation models is limited because they are not designed for this specific task. On the other hand, heuristics-based methods can roughly localize transient distractors but cannot provide accurate segmentation results. By combining heuristics and the segmentation model together, our method takes the best of both worlds and can accurately segment transient distractors from static scenes without any prior knowledge.

Verification of Observation 1. Please see the supplementary materials for additional experiments in which we verify the correctness of Observation 1.

5.4. Ablation Study

Based on Nerfacto, we remove different components of our method to study their effects on two different datasets. As shown in Fig. 10, method (a) without any static maps, *i.e.*, the native Nerfacto, performs the worst. Using SfM-based heuristics or residual-based heuristics alone has limited improvement because the former cannot capture smooth surfaces and the latter has difficulty handling high-frequency details. The complete method (f), which combines them with the segmentation model, achieves the best results.

	$\mathcal{H}^{SfM}$	$\mathcal{H}^{CR}$	SAM	Kubric (Avg.) PSNR↑	Kubric (Avg.) SSIM↑	Kubric (Avg.) LPIPS↓	Distractor (Avg.) PSNR↑	Distractor (Avg.) SSIM↑	Distractor (Avg.) LPIPS↓
(a)	-	-	-	29.76	.861	.210	22.06	.692	.241
(b)	✓	-	-	38.14	.962	.054	**25.67**	**.788**	**.108**
(c)	-	✓	-	39.86	**.967**	**.036**	24.95	.767	.146
(d)	-	✓	✓	**40.12**	**.968**	**.033**	24.58	.779	.126
(e)	✓	✓	-	**40.11**	**.968**	**.035**	**25.40**	**.786**	**.116**
(f)	✓	✓	✓	**40.40**	**.969**	**.033**	**25.66**	**.791**	**.106**

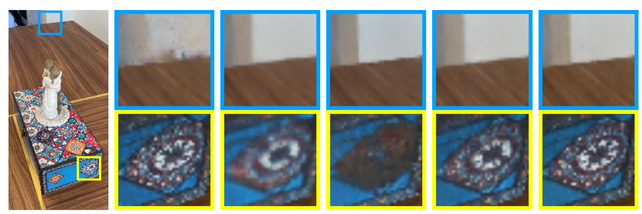
Test Image (b) (c) (d) (e) (f)

Figure 10. **Ablation results.** The patches in blue frames denote the smooth wall, and those in yellow frames denote complex textures. The **1st**, **2nd** and **3rd** best results are highlighted.

6. Conclusions

In this work, we propose a novel heuristics-guided segmentation paradigm that effectively addresses the prevalent issue of transient distractors in real-world NeRF training. By strategically combining the complementary strengths of hand-crafted heuristics and state-of-the-art semantic segmentation models, our method achieves highly accurate segmentation of transient distractors across diverse scenes without any prior knowledge. Through meticulous heuristic design, our method can capture both high and low-frequency static scene elements robustly. Extensive experiments demonstrate the superiority of our approach over existing methods. Please see the supplementary details for **limitations and future work**.

References

[1] Jonathan T Barron, Ben Mildenhall, Matthew Tancik, Peter Hedman, Ricardo Martin-Brualla, and Pratul P Srinivasan. Mip-nerf: A multiscale representation for anti-aliasing neural radiance fields. In *Proceedings of the IEEE/CVF International Conference on Computer Vision*, pages 5855–5864, 2021. 2

[2] Jonathan T Barron, Ben Mildenhall, Dor Verbin, Pratul P Srinivasan, and Peter Hedman. Mip-nerf 360: Unbounded anti-aliased neural radiance fields. In *Proceedings of the IEEE/CVF Conference on Computer Vision and Pattern Recognition*, pages 5470–5479, 2022. 6, 7, 1, 2

[3] Jonathan T Barron, Ben Mildenhall, Dor Verbin, Pratul P Srinivasan, and Peter Hedman. Zip-nerf: Anti-aliased grid-based neural radiance fields. *arXiv preprint arXiv:2304.06706*, 2023. 2

[4] Mathilde Caron, Hugo Touvron, Ishan Misra, Hervé Jégou, Julien Mairal, Piotr Bojanowski, and Armand Joulin. Emerging properties in self-supervised vision transformers. In *Proceedings of the IEEE/CVF international conference on computer vision*, pages 9650–9660, 2021. 8, 3

[5] Pierre Charbonnier, Laure Blanc-Feraud, Gilles Aubert, and Michel Barlaud. Two deterministic half-quadratic regularization algorithms for computed imaging. In *Proceedings of 1st international conference on image processing*, pages 168–172. IEEE, 1994. 3

[6] Liang-Chieh Chen, Yukun Zhu, George Papandreou, Florian Schroff, and Hartwig Adam. Encoder-decoder with atrous separable convolution for semantic image segmentation. In *Proceedings of the European conference on computer vision (ECCV)*, pages 801–818, 2018. 8, 2

[7] Xingyu Chen, Qi Zhang, Xiaoyu Li, Yue Chen, Ying Feng, Xuan Wang, and Jue Wang. Hallucinated neural radiance fields in the wild. In *Proceedings of the IEEE/CVF Conference on Computer Vision and Pattern Recognition*, pages 12943–12952, 2022. 2, 6, 7, 8, 1, 3

[8] Bowen Cheng, Ishan Misra, Alexander G Schwing, Alexander Kirillov, and Rohit Girdhar. Masked-attention mask transformer for universal image segmentation. In *Proceedings of the IEEE/CVF conference on computer vision and pattern recognition*, pages 1290–1299, 2022. 8, 2

[9] MMSegmentation Contributors. MMSegmentation: Openmmlab semantic segmentation toolbox and benchmark, 2020. 3

[10] Chen Gao, Ayush Saraf, Johannes Kopf, and Jia-Bin Huang. Dynamic view synthesis from dynamic monocular video. In *Proceedings of the IEEE/CVF International Conference on Computer Vision*, pages 5712–5721, 2021. 2

[11] Klaus Greff, Francois Belletti, Lucas Beyer, Carl Doersch, Yilun Du, Daniel Duckworth, David J Fleet, Dan Gnanapragasam, Florian Golemo, Charles Herrmann, et al. Kubric: A scalable dataset generator. In *Proceedings of the IEEE/CVF Conference on Computer Vision and Pattern Recognition*, pages 3749–3761, 2022. 5

[12] Mert Asim Karaoglu, Hannah Schieber, Nicolas Schischka, Melih Görgülü, Florian Grötzner, Alexander Ladikos, Daniel Roth, Nassir Navab, and Benjamin Busam. Dynamon: Motion-aware fast and robust camera localization for dynamic nerf, 2023. 2

[13] Bernhard Kerbl, Georgios Kopanas, Thomas Leimkühler, and George Drettakis. 3d gaussian splatting for real-time radiance field rendering. *ACM Transactions on Graphics*, 42 (4):1–14, 2023. 3

[14] Justin Kerr, Chung Min Kim, Ken Goldberg, Angjoo Kanazawa, and Matthew Tancik. Lerf: Language embedded radiance fields. *arXiv preprint arXiv:2303.09553*, 2023. 1

[15] Injae Kim, Minhyuk Choi, and Hyunwoo J. Kim. Up-nerf: Unconstrained pose-prior-free neural radiance fields. *arXiv:2311.03784*, 2023. 2

[16] Alexander Kirillov, Eric Mintun, Nikhila Ravi, Hanzi Mao, Chloe Rolland, Laura Gustafson, Tete Xiao, Spencer Whitehead, Alexander C Berg, Wan-Yen Lo, et al. Segment anything. *arXiv preprint arXiv:2304.02643*, 2023. 2, 4, 5, 7, 8, 1, 3

[17] Jaewon Lee, Injae Kim, Hwan Heo, and Hyunwoo J Kim. Semantic-aware occlusion filtering neural radiance fields in the wild. *arXiv preprint arXiv:2303.03966*, 2023. 2, 3

[18] Peihao Li, Shaohui Wang, Chen Yang, Bingbing Liu, Weichao Qiu, and Haoqian Wang. Nerf-ms: Neural radiance fields with multi-sequence. In *Proceedings of the IEEE/CVF International Conference on Computer Vision*, pages 18591–18600, 2023. 2

[19] Tianye Li, Mira Slavcheva, Michael Zollhoefer, Simon Green, Christoph Lassner, Changil Kim, Tanner Schmidt, Steven Lovegrove, Michael Goesele, Richard Newcombe, et al. Neural 3d video synthesis from multi-view video. In *Proceedings of the IEEE/CVF Conference on Computer Vision and Pattern Recognition*, pages 5521–5531, 2022. 2

[20] Yuan Li, Zhi-Hao Lin, David Forsyth, Jia-Bin Huang, and Shenlong Wang. Climatenerf: Extreme weather synthesis in neural radiance field. In *Proceedings of the IEEE/CVF International Conference on Computer Vision*, pages 3227–3238, 2023. 3

[21] Zhengqi Li, Simon Niklaus, Noah Snavely, and Oliver Wang. Neural scene flow fields for space-time view synthesis of dynamic scenes. In *Proceedings of the IEEE/CVF Conference on Computer Vision and Pattern Recognition*, pages 6498–6508, 2021. 2

[22] Zhaoshuo Li, Thomas Müller, Alex Evans, Russell H Taylor, Mathias Unberath, Ming-Yu Liu, and Chen-Hsuan Lin. Neuralangelo: High-fidelity neural surface reconstruction. In *Proceedings of the IEEE/CVF Conference on Computer Vision and Pattern Recognition*, pages 8456–8465, 2023. 1

[23] Chen-Hsuan Lin, Jun Gao, Luming Tang, Towaki Takikawa, Xiaohui Zeng, Xun Huang, Karsten Kreis, Sanja Fidler, Ming-Yu Liu, and Tsung-Yi Lin. Magic3d: High-resolution text-to-3d content creation. In *Proceedings of the IEEE/CVF Conference on Computer Vision and Pattern Recognition*, pages 300–309, 2023. 1

[24] Haotong Lin, Qianqian Wang, Ruojin Cai, Sida Peng, Hadar Averbuch-Elor, Xiaowei Zhou, and Noah Snavely. Neural scene chronology. In *Proceedings of the IEEE/CVF Conference on Computer Vision and Pattern Recognition*, pages 20752–20761, 2023. 3

[25] Shilong Liu, Zhaoyang Zeng, Tianhe Ren, Feng Li, Hao Zhang, Jie Yang, Chunyuan Li, Jianwei Yang, Hang Su, Jun Zhu, et al. Grounding dino: Marrying dino with grounded pre-training for open-set object detection. *arXiv preprint arXiv:2303.05499*, 2023. 8, 3

[26] Yu-Lun Liu, Chen Gao, Andreas Meuleman, Hung-Yu Tseng, Ayush Saraf, Changil Kim, Yung-Yu Chuang, Johannes Kopf, and Jia-Bin Huang. Robust dynamic radiance fields. In *Proceedings of the IEEE/CVF Conference on Computer Vision and Pattern Recognition*, pages 13–23, 2023. 2

[27] David G Lowe. Distinctive image features from scale-invariant keypoints. *International journal of computer vision*, 60:91–110, 2004. 7

[28] Ricardo Martin-Brualla, Noha Radwan, Mehdi SM Sajjadi, Jonathan T Barron, Alexey Dosovitskiy, and Daniel Duckworth. Nerf in the wild: Neural radiance fields for unconstrained photo collections. In *Proceedings of the IEEE/CVF Conference on Computer Vision and Pattern Recognition*, pages 7210–7219, 2021. 2, 4, 5, 6, 7, 8, 1

[29] Ben Mildenhall, Pratul P Srinivasan, Matthew Tancik, Jonathan T Barron, Ravi Ramamoorthi, and Ren Ng. Nerf: Representing scenes as neural radiance fields for view synthesis. In *European Conference on Computer Vision*, pages 405–421. Springer, 2020. 1, 2, 7

[30] Ben Mildenhall, Dor Verbin, Pratul P. Srinivasan, Peter Hedman, Ricardo Martin-Brualla, and Jonathan T. Barron. MultiNeRF: A Code Release for Mip-NeRF 360, Ref-NeRF, and RawNeRF, 2022. 2

[31] Ashkan Mirzaei, Tristan Aumentado-Armstrong, Konstantinos G Derpanis, Jonathan Kelly, Marcus A Brubaker, Igor Gilitschenski, and Alex Levinshtein. Spin-nerf: Multiview segmentation and perceptual inpainting with neural radiance fields. In *Proceedings of the IEEE/CVF Conference on Computer Vision and Pattern Recognition*, pages 20669–20679, 2023. 3, 5

[32] Thomas Müller, Alex Evans, Christoph Schied, and Alexander Keller. Instant neural graphics primitives with a multiresolution hash encoding. *ACM Transactions on Graphics (ToG)*, 41(4):1–15, 2022. 2

[33] Michael Niemeyer and Andreas Geiger. Giraffe: Representing scenes as compositional generative neural feature fields. In *Proceedings of the IEEE/CVF Conference on Computer Vision and Pattern Recognition*, pages 11453–11464, 2021. 1

[34] Keunhong Park, Utkarsh Sinha, Jonathan T Barron, Sofien Bouaziz, Dan B Goldman, Steven M Seitz, and Ricardo Martin-Brualla. Nerfies: Deformable neural radiance fields. In *Proceedings of the IEEE/CVF International Conference on Computer Vision*, pages 5865–5874, 2021. 2

[35] Sungheon Park, Minjung Son, Seokhwan Jang, Young Chun Ahn, Ji-Yeon Kim, and Nahyup Kang. Temporal interpolation is all you need for dynamic neural radiance fields. In *Proceedings of the IEEE/CVF Conference on Computer Vision and Pattern Recognition*, pages 4212–4221, 2023. 2

[36] Ben Poole, Ajay Jain, Jonathan T Barron, and Ben Mildenhall. Dreamfusion: Text-to-3d using 2d diffusion. In *The Eleventh International Conference on Learning Representations*, 2022. 1

[37] Chen Quei-An. Nerf_pl: a pytorch-lightning implementation of nerf, 2020. 2

[38] Konstantinos Rematas, Andrew Liu, Pratul P Srinivasan, Jonathan T Barron, Andrea Tagliasacchi, Thomas Funkhouser, and Vittorio Ferrari. Urban radiance fields. In *Proceedings of the IEEE/CVF Conference on Computer Vision and Pattern Recognition*, pages 12932–12942, 2022. 2

[39] Viktor Rudnev, Mohamed Elgharib, William Smith, Lingjie Liu, Vladislav Golyanik, and Christian Theobalt. Nerf for outdoor scene relighting. In *European Conference on Computer Vision*, pages 615–631. Springer, 2022. 3

[40] Sara Sabour, Suhani Vora, Daniel Duckworth, Ivan Krasin, David J Fleet, and Andrea Tagliasacchi. Robustnerf: Ignoring distractors with robust losses. In *Proceedings of the IEEE/CVF Conference on Computer Vision and Pattern Recognition*, pages 20626–20636, 2023. 2, 4, 5, 6, 7, 8, 1

[41] Johannes L Schonberger and Jan-Michael Frahm. Structure-from-motion revisited. In *Proceedings of the IEEE conference on computer vision and pattern recognition*, pages 4104–4113, 2016. 7

[42] Yawar Siddiqui, Lorenzo Porzi, Samuel Rota Bulò, Norman Müller, Matthias Nießner, Angela Dai, and Peter Kontschieder. Panoptic lifting for 3d scene understanding with neural fields. In *Proceedings of the IEEE/CVF Conference on Computer Vision and Pattern Recognition*, pages 9043–9052, 2023. 1

[43] Jiaming Sun, Xi Chen, Qianqian Wang, Zhengqi Li, Hadar Averbuch-Elor, Xiaowei Zhou, and Noah Snavely. Neural 3d reconstruction in the wild. In *ACM SIGGRAPH 2022 Conference Proceedings*, pages 1–9, 2022. 1, 2, 3

[44] Roman Suvorov, Elizaveta Logacheva, Anton Mashikhin, Anastasia Remizova, Arsenii Ashukha, Aleksei Silvestrov, Naejin Kong, Harshith Goka, Kiwoong Park, and Victor Lempitsky. Resolution-robust large mask inpainting with fourier convolutions. In *Proceedings of the IEEE/CVF winter conference on applications of computer vision*, pages 2149–2159, 2022. 5

[45] Matthew Tancik, Vincent Casser, Xinchen Yan, Sabeek Pradhan, Ben Mildenhall, Pratul P Srinivasan, Jonathan T Barron, and Henrik Kretzschmar. Block-nerf: Scalable large scene neural view synthesis. In *Proceedings of the IEEE/CVF Conference on Computer Vision and Pattern Recognition*, pages 8248–8258, 2022. 2

[46] Matthew Tancik, Ethan Weber, Evonne Ng, Ruilong Li, Brent Yi, Terrance Wang, Alexander Kristoffersen, Jake Austin, Kamyar Salahi, Abhik Ahuja, et al. Nerfstudio: A modular framework for neural radiance field development. In *ACM SIGGRAPH 2023 Conference Proceedings*, pages 1–12, 2023. 2, 4, 5, 6, 7, 1

[47] Haithem Turki, Deva Ramanan, and Mahadev Satyanarayanan. Mega-nerf: Scalable construction of large-scale nerfs for virtual fly-throughs. In *Proceedings of the IEEE/CVF Conference on Computer Vision and Pattern Recognition*, pages 12922–12931, 2022. 2

[48] Peng Wang, Lingjie Liu, Yuan Liu, Christian Theobalt, Taku Komura, and Wenping Wang. Neus: Learning neural implicit surfaces by volume rendering for multi-view recon-

struction. *Advances in Neural Information Processing Systems*, 34:27171–27183, 2021. 1

[49] Yuang Wang, Xingyi He, Sida Peng, Haotong Lin, Hujun Bao, and Xiaowei Zhou. Autorecon: Automated 3d object discovery and reconstruction. In *Proceedings of the IEEE/CVF Conference on Computer Vision and Pattern Recognition*, pages 21382–21391, 2023. 3

[50] Zhou Wang, Alan C Bovik, Hamid R Sheikh, and Eero P Simoncelli. Image quality assessment: from error visibility to structural similarity. *IEEE transactions on image processing*, 13(4):600–612, 2004. 7

[51] Zian Wang, Tianchang Shen, Jun Gao, Shengyu Huang, Jacob Munkberg, Jon Hasselgren, Zan Gojcic, Wenzheng Chen, and Sanja Fidler. Neural fields meet explicit geometric representations for inverse rendering of urban scenes. In *Proceedings of the IEEE/CVF Conference on Computer Vision and Pattern Recognition*, pages 8370–8380, 2023. 3

[52] Silvan Weder, Guillermo Garcia-Hernando, Aron Monszpart, Marc Pollefeys, Gabriel J Brostow, Michael Firman, and Sara Vicente. Removing objects from neural radiance fields. In *Proceedings of the IEEE/CVF Conference on Computer Vision and Pattern Recognition*, pages 16528–16538, 2023. 5

[53] Tianhao Wu, Fangcheng Zhong, Andrea Tagliasacchi, Forrester Cole, and Cengiz Oztireli. D2nerf: Self-supervised decoupling of dynamic and static objects from a monocular video. *Advances in Neural Information Processing Systems*, 35:32653–32666, 2022. 2, 5, 6, 7, 8, 1

[54] Yiheng Xie, Towaki Takikawa, Shunsuke Saito, Or Litany, Shiqin Yan, Numair Khan, Federico Tombari, James Tompkin, Vincent Sitzmann, and Srinath Sridhar. Neural fields in visual computing and beyond. In *Computer Graphics Forum*, pages 641–676. Wiley Online Library, 2022. 1

[55] Youtan Yin, Zhoujie Fu, Fan Yang, and Guosheng Lin. Ornerf: Object removing from 3d scenes guided by multiview segmentation with neural radiance fields. *arXiv preprint arXiv:2305.10503*, 2023. 3, 5

[56] Kai Zhang, Gernot Riegler, Noah Snavely, and Vladlen Koltun. Nerf++: Analyzing and improving neural radiance fields. *arXiv preprint arXiv:2010.07492*, 2020. 2

[57] Richard Zhang, Phillip Isola, Alexei A Efros, Eli Shechtman, and Oliver Wang. The unreasonable effectiveness of deep features as a perceptual metric. In *Proceedings of the IEEE conference on computer vision and pattern recognition*, pages 586–595, 2018. 7

[58] Shuaifeng Zhi, Tristan Laidlow, Stefan Leutenegger, and Andrew J Davison. In-place scene labelling and understanding with implicit scene representation. In *Proceedings of the IEEE/CVF International Conference on Computer Vision*, pages 15838–15847, 2021. 1

[59] Bolei Zhou, Hang Zhao, Xavier Puig, Tete Xiao, Sanja Fidler, Adela Barriuso, and Antonio Torralba. Semantic understanding of scenes through the ade20k dataset. *International Journal of Computer Vision*, 127:302–321, 2019. 3